

---

# Design and Performance of a Selectable-Rate Streak-Camera Deflection Ramp Generator

## Introduction

Electro-optic streak cameras have been used at LLE for many years to resolve high-bandwidth, low-repetition-rate, pulsed laser phenomena. Until now the sweep rate was governed by a fixed-rate voltage ramp generator used to drive the sweep deflection plates.

Altering the time base required physically changing the ramp generator. In this article a new method of generating the sweep deflection ramps is presented that permits changing the sweep rate by computer control without replacing the ramp generator. A logic level signal can now be used to change sweep rates without the need for invasive component changes. This new development permits fast and easy sweep rate changes for streak cameras in any location throughout the laboratory, especially in low accessibility locations such as clean rooms and high-power-laser environments.

As a result of this work, a 50- $\Omega$  matched-impedance voltage ramp generator was developed. The matched-impedance design of the generator allows the deflection signals to propagate on standard 50- $\Omega$  coaxial cable without distortion of the ramp waveform regardless of cable length. The ramp generator's location and interconnect length to the deflection plates are less restricted than with the previous design. In situations where access to the streak camera's tube deflection electrodes is limited by space or environmental constraints, this feature can be a great asset.

The first production circuit has been installed in an infrared-sensitive streak camera, and tests have been performed to measure sweep rate and linearity. The infrared camera contains a Phillips P510 streak tube<sup>1</sup> coupled to a 512  $\times$  512-pixel CCD. The circuit is designed with four selectable sweep ramp rates, which produce voltage ramps of  $\pm 1000$  V in 2, 6, 10, and 20 ns. Measured results agree well with design modeling.

## Background

The LLE streak camera used for this work contains two deflection plates that are differentially driven by two equal

but opposite-polarity voltage ramp signals. Throughout this discussion only one of the ramp generators will be described. It is assumed that the other ramp generator uses the same technology and produces the same result with the opposite-polarity voltage.

The original streak-camera ramp generator designs at LLE were based on a resistor, inductor, capacitor (RLC) resonator.<sup>2</sup> The resonator, when driven by a voltage-step waveform, produced a damped sinusoidal response. The voltage step was produced by switching a fast avalanche transistor stack. Proper selection of the resonant frequency (the frequency where the capacitive reactance equals the inductive reactance) and the resistive damping factor produced a voltage ramp with the desired sweep slope. Closed-form expressions and computer simulations were developed to determine the required values of the resonator components for a specified sweep ramp. The basic circuit configuration is illustrated in Fig. 85.15.

The RLC ramp generator had several shortcomings: In the RLC circuit the values of the rate-determining reactances are small enough that parasitic reactances, such as those introduced by electromechanical relay contacts and deflection-plate feed lines, can greatly affect the sweep ramp characteristics. For this reason a selectable-rate ramp generator could not be

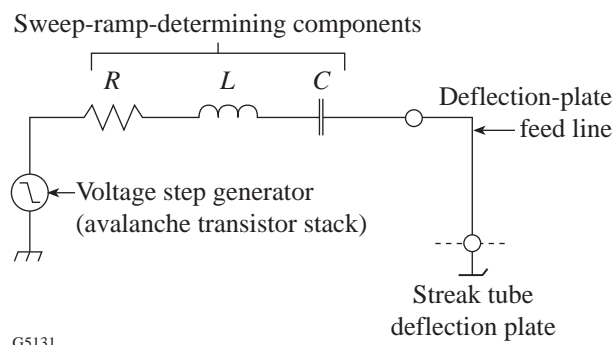


Figure 85.15  
Original RLC resonator streak-camera ramp generator design.

designed using the RLC circuit configuration. To change ramp rates, removal and replacement of the RLC ramp generator module was required. For many this limitation was both time consuming and inconvenient.

Another disadvantage of the RLC resonator approach was that the feed line between the ramp generator and the deflection plate connection forms part of the RLC resonant circuit. A feed line that is too long or physically positioned improperly will distort the ramp shape significantly. As a result the ramp generator had to be mounted as close as physically possible to the streak tube deflection plate connections. In streak cameras where space around the tube deflection plate connections is limited, this complicates the overall design of the instrument.

The limitations of the RLC base ramp were overcome by a new sweep ramp generator design. The new design is a matched low-impedance ramp generator. With the low-impedance design, small shunt impedance parasitics, such as relay capacitance and feed line parasitics, have a negligible effect on the sweep ramp shape. Matching the impedance of the generator to the load removes the problems associated with the feed lines. Theoretically, the input impedance of an ideal transmission line terminated in its characteristic impedance is equal to the characteristic impedance regardless of line length. Thus the matched impedance ramp generator will produce the same waveform regardless of the interconnection length between the generator and the deflection plates as long as the generator, cable, and termination are of matched impedance.

The step generator needed for the matched-impedance ramp generator must be able to withstand higher switching

current than the step generator for the RLC resonator. An avalanche transistor stack alone will not withstand the step current for a long enough duration when driving a 50-Ω load.<sup>3</sup> The step current duration must be long enough to maintain the step voltage at a specific potential following the active portion of the sweep to avoid retrace problems prior to camera shutter closure. In addition a matched generator and load will divide the switching potential, one half across the step generator internal impedance with the other half developed across the load. For a matched generator a higher voltage step is required to produce the same ramp voltage as developed by the RLC resonator approach.

**Multi-rate Network**

The block diagram of the selectable-rate streak-camera deflection ramp generator is illustrated in Fig. 85.16. The first production ramp generator module is shown in Fig. 85.17. The basic parts of the generator are the matched-impedance (50 Ω) voltage step generator and the filter network that determines the sweep rate.

Details of the low-pass-filter network are illustrated in Fig. 85.18. There are four individual electromechanical relay-selectable, low-pass filters. A remote-control logic interface within the filter network controls the relays. Each filter limits the high-frequency spectral components produced by the step generator, which in turn produces an output sweep ramp at a slower rate. Selection of the low-pass-filter cutoff frequency  $f_c$  determines the produced slope of the ramp. Each filter consists of a three-section inductor/capacitor (LC) passive low-pass circuit. With four filters the generator is capable of four different sweep rates. A fifth filter is included in series with the

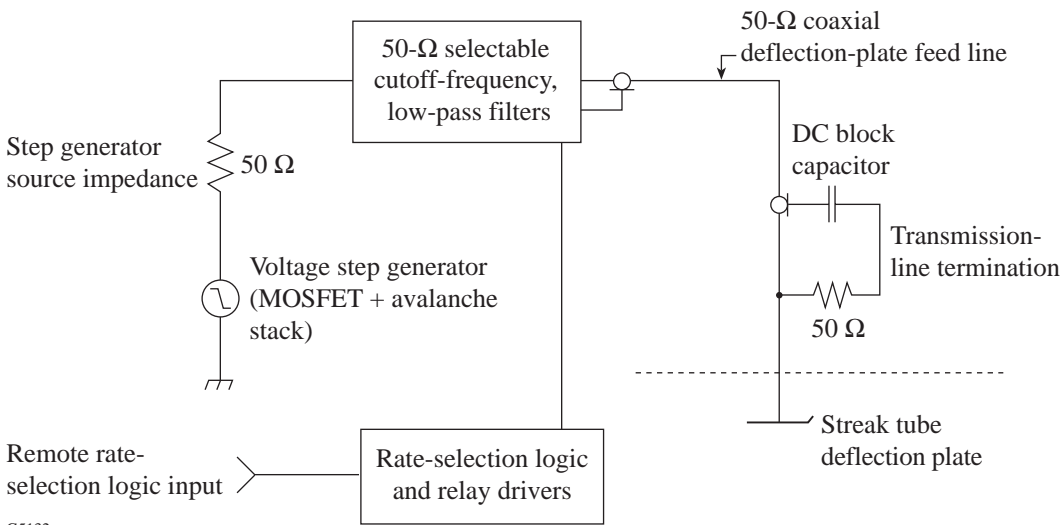


Figure 85.16  
Block diagram of a new selectable-rate streak-camera deflection ramp generator.

selectable filters to limit high-frequency-signal leakage through the four selectable low-pass filters. The cutoff frequency of the fifth filter is set higher than the other filters so their passband performance is not affected.

Each 50-Ω matched-impedance low-pass filter is based on the coefficients that produce a Butterworth characteristic.<sup>4</sup> A Butterworth low-pass filter produces monotonically increasing attenuation with increasing frequency. Closed-form equations are well known relating the component values to the one-half-power, or 3-dB, cutoff frequency  $f_c$ . Equations (1) through (3) provide the formulas required to calculate the component values for the three-section 50-Ω filters:

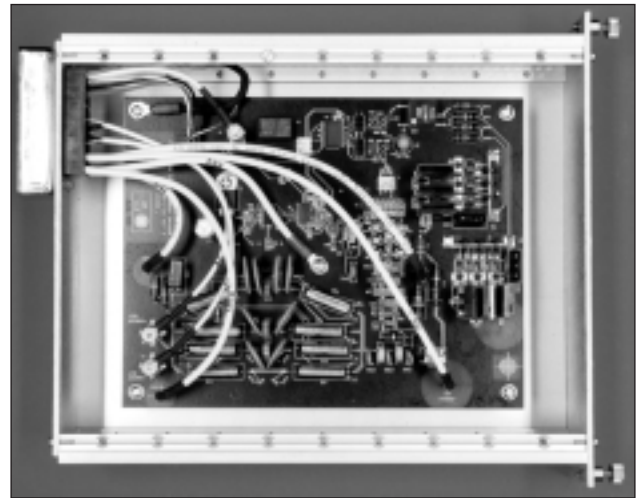
$$\omega_c = 2\pi f_c \tag{1}$$

(low-pass cutoff radian frequency, rad/s)

$$L = 2Z/\omega_c \text{ (henrys),} \tag{2}$$

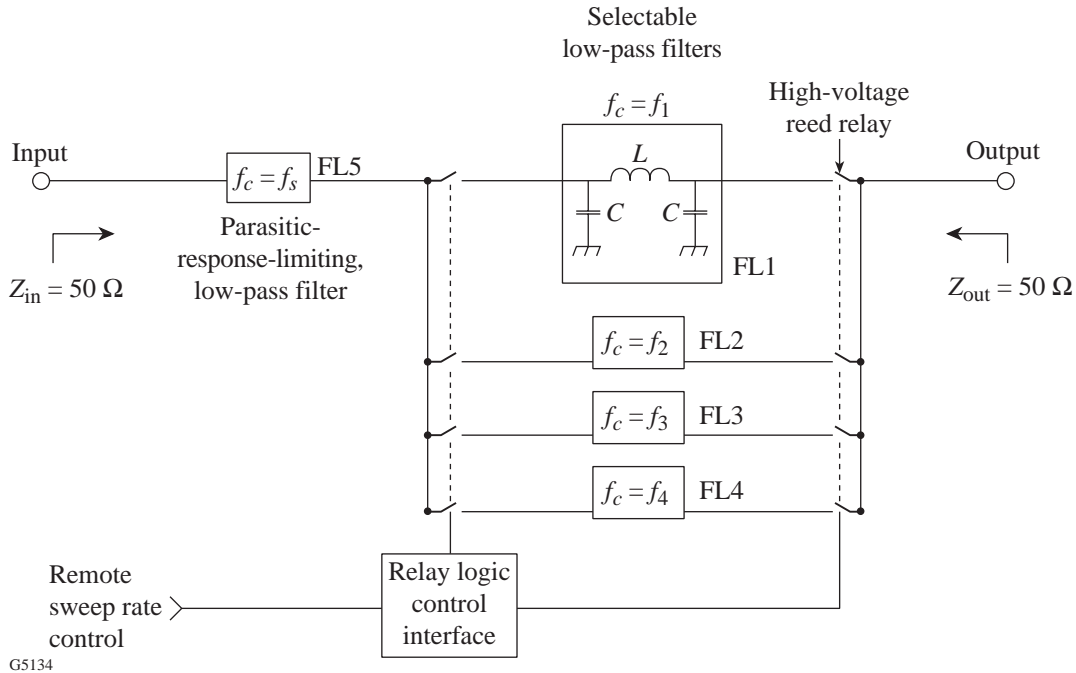
$$C = 1/(\omega_c Z) \text{ (farads),} \tag{3}$$

where  $Z = 50 \Omega$  is the impedance of the filter.



G5133

Figure 85.17 Photograph of the selectable-rate streak-camera deflection ramp generator module. The top side of the board (shown) contains the negative-slope ramp generator, rate-selection logic, and relay drivers. The opposite side of the board (not shown) contains the positive-slope ramp generator.



G5134

Figure 85.18 Block diagram of the 50-Ω selectable cutoff low-pass filters that determine the sweep ramp rate.

A SPICE<sup>5</sup> computer circuit simulation that includes the low-pass filters was developed for the ramp generator. A simplified schematic of the circuit model is shown in Fig. 85.19. Filters with low-pass cutoff frequencies from 1 to 155 MHz were evaluated using the circuit model to determine their effect on the ramp slope. Two parameters are used to relate the effect of the low-pass filter to the ramp slope. The first parameter  $t_r$  is the time required for the voltage ramp to change by 1000 V over its most linear portion. This is the region of the ramp generator's output waveform that produces the sweep deflection over the active region of the streak tube's output window. The second parameter  $K_f$  is the product of  $t_r$  with the low-pass cutoff frequency  $f_c$ . This product is the ratio of the ramp time to the period of the low-pass cutoff frequency. Knowing  $K_f$ , the low-pass cutoff frequency can be calculated for a specific active ramp duration  $t_r$  using

$$f_c = K_f / t_r \tag{4}$$

Figure 85.20 illustrates the relation between the active sweep ramp time  $t_r$  and the constant  $K_f$  as determined through computer modeling. Rearranging and substituting terms from Eq. (4) in Eqs. (2) and (3) leads to the following equations that are needed to determine the values of the low-pass filter components from the value of  $t_r$  and  $K_f$ :

$$L = (2Zt_r) / (2\pi K_f) \text{ (henries),} \tag{5}$$

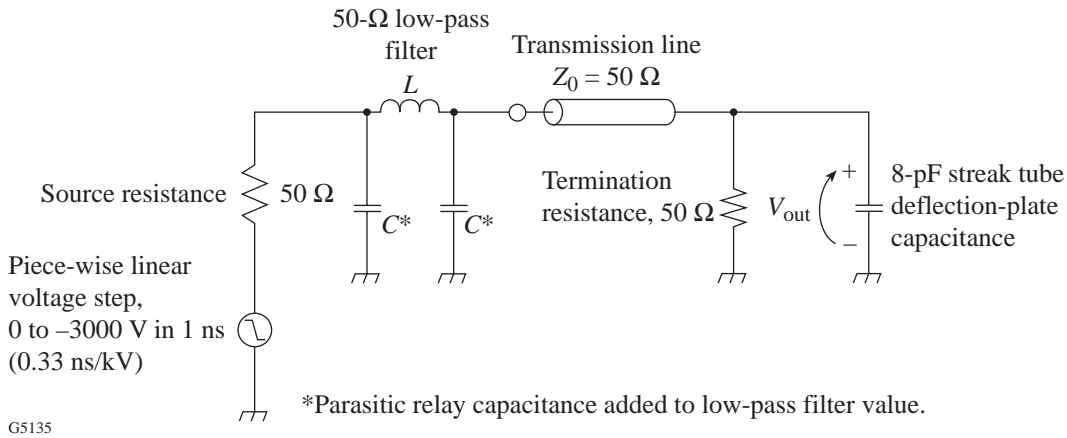
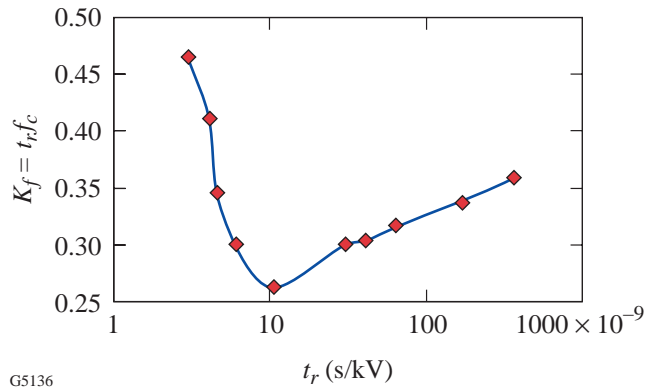


Figure 85.19 Simplified schematic of the SPICE circuit simulation model used to determine a correlation between low-pass-filter cutoff frequency and sweep ramp rate. Actual circuit model contains detailed relay, step generator, and component parasitic models.

$$C = t_r / (2\pi K_f Z) \text{ (farads),} \tag{6}$$

where  $t_r$  = active ramp duration in seconds.

In an ideal step generator the step transition occurs instantaneously. For any practical step generator the step transition is of finite duration. In the SPICE circuit simulation the transition rate for the step generator was chosen to be 0.33 ns/kV. Typically an avalanche transistor stack can produce this ramp rate; however, as stated previously, the avalanche stack cannot



G5136

Figure 85.20 Plot of frequency product constant  $K_f$  as a function of sweep time  $t_r$ . Results produced by SPICE circuit simulation of the selectable-rate ramp generator.

withstand the 30-A switching current for a duration of several microseconds as required for a matched 50- $\Omega$  step generator.<sup>3</sup> High-voltage MOSFET's (metal-oxide silicon field effect transistors) can support a 50- $\Omega$  step generator switching current and voltage but cannot provide a transition rate of 0.33 ns/kV. Typical MOSFET switching speeds are of the order of 3.3 ns/kV. Combining the two switch technologies in parallel provides both the speed and durability required for the 50- $\Omega$  step generator by utilizing the speed of the avalanche transistor switch and the current-handling capabilities of the MOSFET switch. The avalanche transistor switch is triggered first, followed by the MOSFET switch after a short delay. This step generator is illustrated in Fig. 85.21.

The avalanche transistor stack follows a design using a tapered transmission line–matching technique developed at Lawrence Livermore National Laboratory.<sup>6</sup> This technique uses the internal self-inductance of the avalanche transistors combined with added collector-to-ground capacitance chosen to effectively create a transmission line that tapers from a low impedance of several ohms at the bottom to 50  $\Omega$  at the top of the stack. An avalanche stack designed in this manner produces a faster switching rate into 50  $\Omega$  than a conventionally designed stack where impedance matching is not included. The tapered transmission line stack is capable of driving a 50- $\Omega$  load for

short periods (50 ns) with a typical rise time of 0.33 ns/kV. To limit the switching current duration in the avalanche stack, a capacitance of 220 pF is connected in series with the 50- $\Omega$  load. Well before the avalanche transistors are stressed, the series capacitor discharges and reduces the avalanche stack current.

The MOSFET switch is designed to have a switching rate of 3.3 ns/kV with an output matched to 50  $\Omega$  through the use of a series resistor. The MOSFET stack has a lower on-state resistance than 50  $\Omega$ , and the series resistor raises it up to the desired level. This switch is connected in parallel with the avalanche transistor stack. The MOSFET switch is triggered immediately after the avalanche transistor stack and is fully on before the avalanche stack series current-limiting capacitor is discharged. Thus the avalanche transistor stack provides the leading edge of the voltage step, and the MOSFET stack provides the step-holding time to prevent streak camera retrace and avalanche stack degradation. The source impedance of the composite switch is 50  $\Omega$  except for the time interval between the MOSFET switch turn-on and when the avalanche transistor stack series capacitor is fully discharged. This does not produce a measurable effect on the output since any mismatch reflection is terminated at the deflection plate termination and not re-reflected. The composite switch waveform is illustrated in Fig. 85.22.

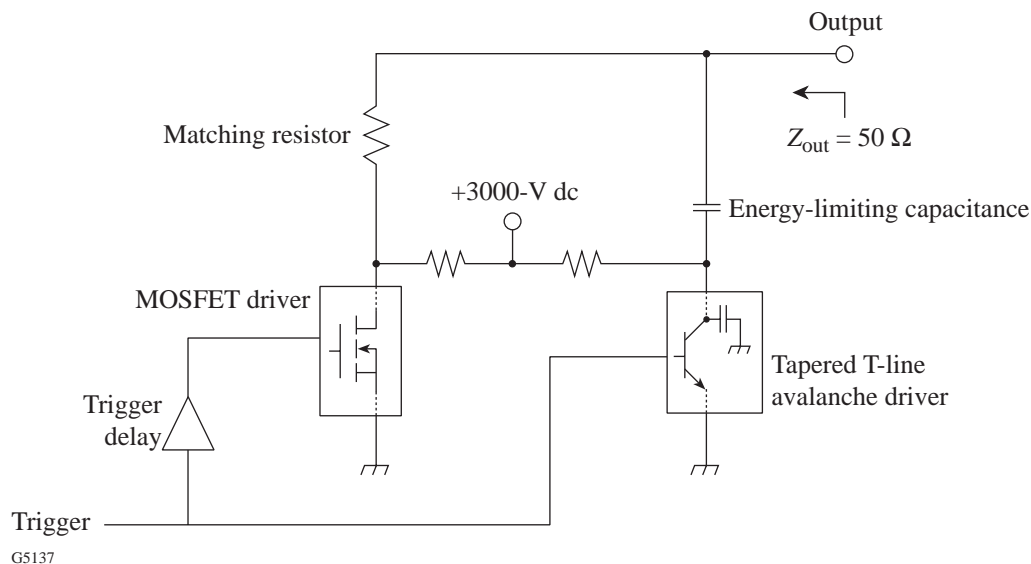


Figure 85.21

Block diagram of the 3000-V composite avalanche transistor stack and MOSFET step generator. The MOSFET driver contains three series-connected, simultaneously triggered 1200-V MOSFET's. The avalanche transistor stack is a ten-level transistor stack designed using the tapered transmission line technique developed at Lawrence Livermore National Laboratory.<sup>6</sup>

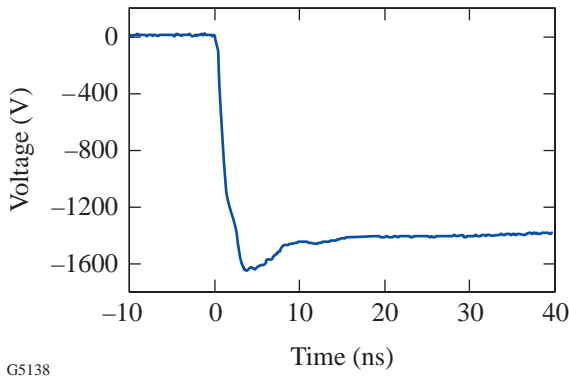


Figure 85.22 Measured output waveform produced by the composite avalanche transistor and MOSFET step generator. Fall time of step is 1 ns/kV.

The composite switch and selectable filter network form the selectable-rate ramp generator. A positive- and negative-voltage pair of these generators are needed to produce a complete differential deflection-plate generator. A 50-Ω transmission line is used to connect the ramp generator to the deflection plates. A matched 50-Ω termination is connected at the deflection-plate end of the transmission line.

**Measured Electrical Performance**

The electrical performance of the selectable-rate ramp generator is summarized in Figs. 85.23 and 85.24 and Table 85.I. In Fig. 85.23 all four sweep waveforms are superimposed. In Table 85.I the design parameters are listed with the measured results for each of the four sweep rates. The measured data for Fig. 85.23 and Table 85.I were recorded using a high-bandwidth oscilloscope<sup>7</sup> and a high-voltage, high-bandwidth probe<sup>8</sup> connected to the deflection plate of the streak tube. In Fig. 85.24 the measured and desired sweep rates for the four different selectable speeds are compared.

The differences between the desired and measured sweep rates indicate that more refinement of the filter factor  $K_f$  must be performed to get a closer correlation between the calculated and measured sweep rates. With an accurate  $K_f$  factor any reasonable sweep rate can be defined, and the appropriate low-pass filter can be designed using Eqs. (5) and (6). Errors in  $K_f$  are generated by incomplete modeling of the actual circuit parasitics in the SPICE computer simulation model for the ramp generator and by non-ideal characteristics of the composite voltage step generator. Since the measured sweep rates may be faster or slower than the desired rates, it should be possible to determine  $K_f$  to a high degree of accuracy with more-accurate computer circuit simulations.

Measurements of the sweep-speed nonlinearity indicate that the deflection rate slope is not uniform across the active sweep. Figure 85.25 illustrates the nonuniformity in the ramp slope for a sweep rate of 4.4 ps/pixel. The sweep rate is generally slow on the edges of the sweep and fast in the center. The measured sweep waveform has a sinusoidal characteristic instead of being a linear ramp. This nonlinearity is produced by the limited summation of sinusoids as theoretically generated by a step response propagated through a low-pass filter. The nonlinearity is reproducible with respect to the sweep waveform timing and should be removable when processing the streak image data. Increasing the ramp generator voltage swing

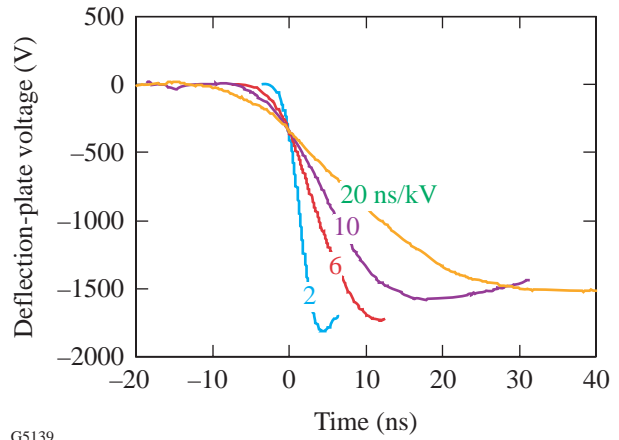


Figure 85.23 Measured output waveforms from the selectable-rate deflection ramp generator. The sweep waveforms for the four different ramp rates are superimposed.

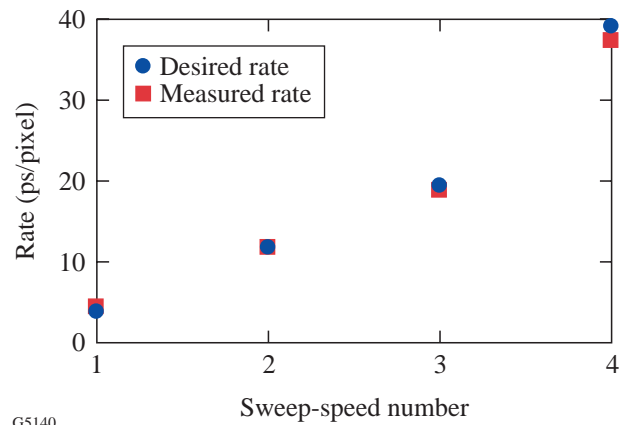


Figure 85.24 Comparison of desired and measured sweep rates.

would reduce the nonlinearity. This would place the active portion of the ramp generator output in an area of the waveform where the slope is more constant. The improved linearity must be traded off with increased complexity of the step generator and low-pass filter networks to accommodate the increased voltages and currents.

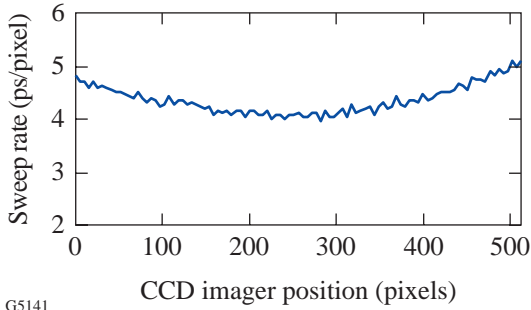


Figure 85.25 Measured sweep rate versus position on the CCD for a 4.4 ps/pixel sweep rate.

### Optical Characterization of the Ramp Generator

A selectable-rate ramp generator was installed in a streak camera and characterized at a designed ramp rate of 17 ps/pixel using a 4.5-ns optical comb pulse.<sup>9</sup> The measurement setup (Fig. 85.26) shows the streak camera input illuminated with the comb pulse and the streak camera’s deflection plate ramp generator triggered from a timing system synchronized with the comb pulse. Since the duration of the comb pulse is less than the sweep time of the ramp generator, the time delay between the ramp generator trigger and the arrival of the comb pulse at the streak camera was varied in order to scan the comb pulse over the full sweep duration. A series of streaks were recorded while changing this delay. The streak camera’s sweep speed was characterized by using the constant time interval between each pair of adjacent peaks within the comb pulse to determine the average sweep dwell time at the center CCD pixel location (Fig. 85.27). By analyzing the acquired streaks of the comb pulse the streak camera’s sweep speed as a function of deflection position, in this case CCD pixel position, was determined and compared to the measurement made by the

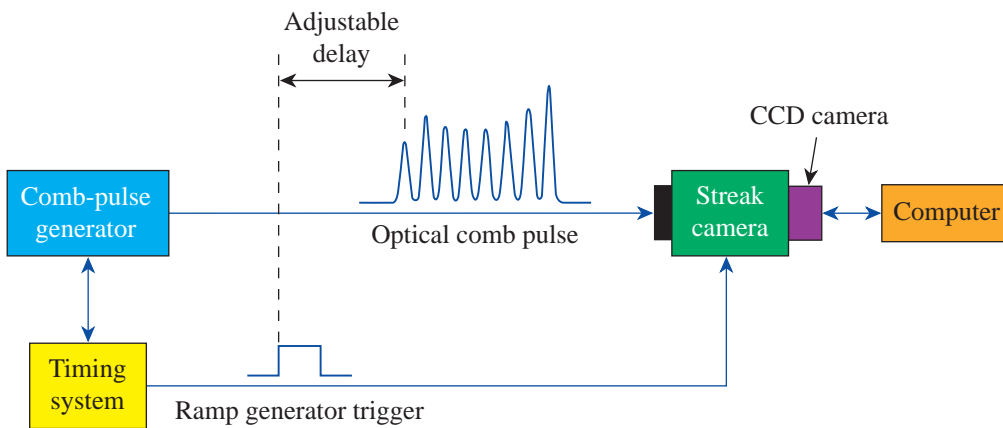


Figure 85.26 The streak camera is illuminated with a 4.5-ns-duration comb pulse, and the deflection-plate ramp generator is triggered from a timing system with an adjustable delay relative to the comb pulse.

Table 85.I: Measured and simulated result comparison for the ramp generator.

Full-Width Sweep Time $t_r$ (ns)	Desired Rate (ps/pixel)	Filter Factor $K_f$	Theoretical Filter $f_c$ (MHz)	Actual Filter $f_c$ (MHz)	Measured Average Rate (ps/pixel)	Measured Rate Deviations from Average (ps/pixel)	
						min	max
2	3.9	0.47	235.0	155.0	4.4	-0.5	0.3
6	11.7	0.30	50.7	50.8	11.6	-1.7	1.1
10	19.5	0.26	26.0	29.3	18.9	-3.6	3.1
20	39.1	0.29	14.5	15.6	37.5	-8.8	7.3

electrical technique discussed earlier (Fig. 85.28). The spacing between the peaks of the comb pulse limits how close to the beginning and end of a streak the sweep speed can be reliably characterized because two adjacent peaks are required to determine the sweep speed at the point midway between them. We have found that for different ramp-rate selections, the electrical characterization of the ramp generator agrees well enough with the optical characterization to allow the initial setup to be done electrically and then perform the final optical characterization using the comb pulse. This will expedite the building and testing of new ramp generators while maintaining the availability of the streak cameras for use with experiments on OMEGA.

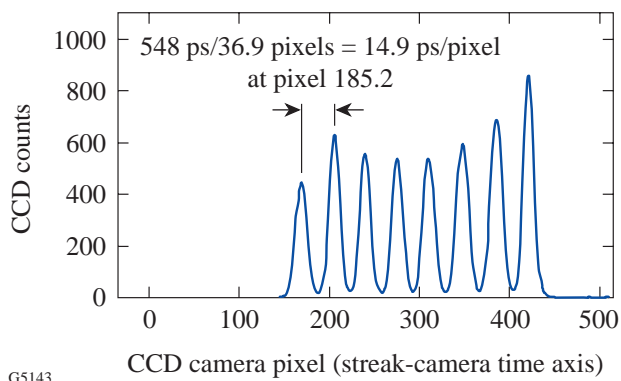


Figure 85.27

The constant time interval between each pair of adjacent peaks within the comb pulse is used to determine the sweep dwell time at the CCD pixel location midway between the peaks.

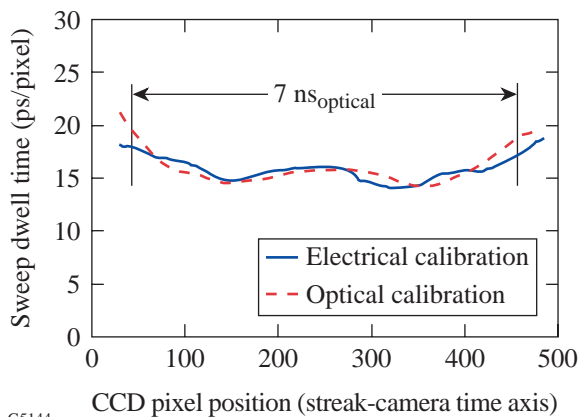


Figure 85.28

The optical and electrical measurements of the ramp generator agree well enough to allow the initial setup to be done electrically and then to perform the final optical characterization using the comb pulse.

## Conclusion

A new method of generating streak-camera deflection ramps utilizing a 50- $\Omega$  composite MOSFET/avalanche transistor step generator and a relay-selectable low-pass-filter network was presented. This new design allows remote selection of four different sweep rates and provides a 50- $\Omega$  interface to the streak tube deflection plates. The 50- $\Omega$  interface relieves the requirement of mounting the ramp generator in close proximity to the deflection plates since the deflection signal can propagate along any length of standard 50- $\Omega$  coaxial cable.

There is good agreement between the modeled and measured sweep rates. The observed differences can be reduced by incorporating a more detailed computer-aided simulation model that accounts for all non-ideal component behavior. The nonlinearity in the ramp rate is reproducible and can be corrected in the data analysis.

## ACKNOWLEDGMENT

This work was supported by the U.S. Department of Energy Office of Inertial Confinement Fusion under Cooperative Agreement No. DE-FC03-92SF19460, the University of Rochester, and the New York State Energy Research and Development Authority. The support of DOE does not constitute an endorsement by DOE of the views expressed in this article.

## REFERENCES

1. P510PSU streak tube, Philips Photonics, Slatersville, RI 02876.
2. Laboratory for Laser Energetics LLE Review **73**, 6, NTIS document No. DOE/SF/19460-212 (1997). Copies may be obtained from the National Technical Information Service, Springfield, VA 22161.
3. Zetex, Inc., Commack, NY 11725.
4. E. C. Jordan, *Reference Data for Engineers: Radio, Electronics, Computer, and Communications*, 7th ed. (H. W. Sams, Indianapolis, IN, 1985), pp. 9-14, 9-19.
5. SPICE 3F2, developed by the Department of Electrical Engineering and Computer Sciences, University of California, Berkeley, CA 94720.
6. E. S. Fulkerson and R. Booth, Lawrence Livermore National Laboratory, Livermore, CA, UCRL-JC-116309 (1994).
7. Oscilloscope Model No. TDS684, Tektronix Corporation, Beaverton, OR 97077.
8. Oscilloscope Probe Model No. P5100, Tektronix, Inc., Wilsonville, OR 97070.
9. Laboratory for Laser Energetics LLE Review **72**, 184, NTIS document No. DOE/SF/19460-199 (1997). Copies may be obtained from the National Technical Information Service, Springfield, VA 22161.